Techno-economic analysis of cryogenic carbon capture process from forest biomass: effects of transportation cost and energy consumption

João Roberto F. S.[a], João P. Pereira[b], Durães L.[c], José B. Ribeiro[d]

[a]Univ de Coimbra, ADAI, Department of Mechanical Engineering, Rua Luís Reis Santos, Pólo II, 3030-788 Coimbra, Portugal, jrfs@uc.pt
[b]Univ de Coimbra, ADAI, Department of Mechanical Engineering, Rua Luís Reis Santos, Pólo II, 3030-788 Coimbra, Portugal, joao.pereira@dem.uc.pt
[c]Univ de Coimbra, CERES, Dept. Chem. Eng., Coimbra, Portugal, luisa@eq.uc.pt
[d]Univ de Coimbra, ADAI, Department of Mechanical Engineering, Rua Luís Reis Santos, Pólo II, 3030-788 Coimbra, Portugal, jose.baranda@dem.uc.pt

Abstract:

The decarbonization of energy systems requires scalable carbon capture solutions, particularly in bioenergy systems capable of delivering negative emissions. However, the feasibility of such systems is largely constrained by the high energy demand and cost of CO_2 separation. While cryogenic CO_2 capture has shown potential for high-purity recovery, existing studies focus mainly on large-scale fossil-based applications and lack consistent techno-economic assessments for biomass-integrated systems. This work addresses this gap by evaluating a forest-residues-fuelled Rankine Cycle (RC) based generation plant coupled with an anti-sublimation cryogenic CO_2 capture unit, considering capacities of 50–500 kt/y through steady-state process simulation, mass and energy balances, and cost modelling based on scaling laws. The system achieves CO_2 capture rates from 1.68 to 16.80 kg/s with a fixed 95% capture efficiency, with energy demand dominated by the capture and dehumidification units (93.2% of total electricity consumption). The gross specific electricity consumption of the process is 726.5 kWh/tCO_2. When accounting for internal electricity generation from biomass combustion, the net electricity demand decreases to 363.1 kWh/tCO_2. Economically, the system is OPEX-driven, with biomass and transportation costs as the main contributors, while eliminating biomass purchase costs reduces OPEX by up to 49 % and carbon capture cost (CCC) by up to 39 %. Sensitivity analysis shows CCC variations up to ± 11 % for biomass moisture and ± 15 % for OPEX, with financial parameters remaining below ± 2 %. These results demonstrate that improving energy efficiency, feedstock quality, and supply logistics is critical for enabling cost-effective decentralized biomass-based cryogenic CO_2 capture systems and advancing negative-emission technologies.

Keywords:

Anti-sublimation; Carbon capture; Forest residues; Techno-economic analysis.

1. Introduction

The decarbonization of energy and industrial systems is a central pillar of global climate mitigation strategies, as highlighted by the Intergovernmental Panel on Climate Change (IPCC), which identifies carbon capture, utilization, and storage (CCUS) as a critical technology for achieving net-zero emissions targets [1]. In parallel, the International Energy Agency (IEA) emphasizes that large-scale deployment of carbon capture will be necessary not only in fossil-based sectors but also in bioenergy systems to enable negative emissions through Bioenergy with Carbon Capture and Storage (BECCS) [2]. Within this framework, forest biomass residues represent a particularly attractive feedstock due to their wide availability, low economic value, contribution to sustainable forest management, and fuel management in forest fire risk zones. When integrated into cogeneration systems, biomass can simultaneously provide heat and electricity while enabling net carbon removal when coupled with CO_2 capture technologies. In addition to permanent removal pathways, biogenic CO_2 recovered from biomass systems may also serve as a feedstock for downstream e-fuel synthesis when combined with green hydrogen [3]. However, the overall feasibility of such systems is strongly constrained by the performance, energy demand, and cost of the CO_2 separation stage, which typically dominates both the energy penalty and the techno-economic performance of the process.

The current state of research on cryogenic CO_2 capture technologies, summarized in Table 1, shows a wide range of system configurations, including anti-sublimation, distillation, and liquefaction processes. Among these, anti-sublimation systems have been extensively investigated, with reported Specific Energy Consumption (SEC) values typically ranging from 200 to 300 kWh/t_{CO_2} under optimized conditions, but reaching significantly higher values (up to 600 – 1200 kWh/t_{CO_2}) depending on operating conditions and CO_2 concentration [4 - 6]. Distillation-based systems generally exhibit lower SEC values (100 – 170 kWh/t_{CO_2}) and competitive capture costs (13 – 39 €/t_{CO_2}), although often at the expense of higher capital intensity and process complexity [7], [8]. Liquefaction systems present intermediate performance, with SEC values around 110 – 160 kWh/t_{CO_2} [9], [10]. Despite these advances, the literature reveals significant variability in reported techno-economic indicators, limited consistency in system boundaries, and a strong dependence of performance on scale and flue gas conditions. Moreover, most studies focus on fossil-based systems or large-scale centralized plants, with comparatively limited attention given to transportation costs, biomass-based configurations and integrated combustion and Rankine cycle systems.

***Table 1**. Key performance indicators of cryogenic CO_2 capture technologies.*

Cryogenic System	Capture cost, €/t_{CO_2}	Capture SEC, kWh/t_{CO_2}	CAPEX, M€	OPEX, M€/y	Capacity, kg/s	Ref.
Anti-sublimation	-	231.7–245.6	-	-	75.6	[4]
Anti-sublimation	14.46–39.16	201.1–232.8	160.58	14.67–47.72	62.6	[11]
Anti-sublimation	-	111.1–311.4	-	-	-	[12]
Anti-sublimation	34.82	278	-	-	8.44	[13]
Anti-sublimation	-	608.3–672.2	-	-	600	[5]
Anti-sublimation	-	305.6–361.1	-	-	-	[14]
Anti-sublimation	-	500	-	-	-	[15]
Anti-sublimation	45.85	301.8	299.56	61.95	125	[6]
Distillation	13.15–22.83	103–172	26.52–58.81	19.60–41.51	68.5–91.3	[7]
Distillation	35.77–37.25	148–164	833.55	-	97.2	[16]
Distillation	27.95–38.85	127.9–160.9	23.2–57.1	-	32.5	[8]
Liquefaction	-	120–140	-	-	124.2	[9]
Liquefaction	-	111.4	106.69	35.56	0.0405	[10]

In this context, the present work addresses the identified limitations in the literature, namely the variability in techno-economic indicators and the limited consideration of biomass-based, decentralized combustion systems with integrated logistics by performing a techno-economic analysis of a forest-residues-fuelled Rankine Cycle (RC) based generation plant integrated with a cryogenic CO_2 capture unit based on anti-sublimation. The study evaluates the influence of plant scale, energy consumption, and biomass acquisition and transportation costs on the overall carbon capture cost (CCC), considering processing capacities ranging from 50 to 500 kt/y. The process model is developed under steady-state conditions, combining mass and energy balances with cost correlations and scaling laws to capture both technical and economic behaviour. By explicitly linking process performance with economic outcomes, this work provides insight into the feasibility of decentralized biogenic carbon capture systems and identifies key drivers for cost reduction, particularly in relation to energy efficiency and logistics. The results contribute to the understanding of cryogenic capture integration in bioenergy systems and support the development of scalable negative-emission technologies.

2. Methodology

2.1. Process Description

The system under study consists of a forest-residues-based cogeneration plant integrated with a cryogenic CO_2 capture unit, as illustrated in Figure 1. The process includes biomass pre-treatment, combustion, flue gas cleaning, and CO_2 separation. All simulations were performed under steady-state conditions for four plant capacities of 50, 100, 200, and 500 kt/y of wet biomass input.

Forest residues are first subjected to size reduction in a grinding unit to ensure a suitable particle size for downstream processing. The biomass is then dried to reduce moisture content, improving combustion efficiency and reducing energy losses associated with water evaporation. The dried biomass is fed into a combustion boiler, where it is oxidized with excess air to produce high-temperature flue gases and thermal energy.

The thermal energy released during combustion is partially recovered as useful heat, which is used to supply the drying unit. The remaining thermal energy is converted into electricity via a steam turbine-generator system. The generated electricity is used to meet internal process demands, with any deficit supplied from the grid or surplus exported.

The flue gas produced in the boiler undergoes sequential cleaning steps. Particulate matter is removed using a bag filter, followed by desulphurization to reduce SO_2, which is critical for equipment lifetime [17]. The gas stream is then cooled and partially dehumidified to condense water vapour, improving the efficiency of downstream CO_2 separation.

Finally, the conditioned flue gas is fed into a cryogenic CO_2 capture unit based on anti-sublimation, where CO_2 is separated and recovered as a solid high-purity product stream. The remaining gases are vented.

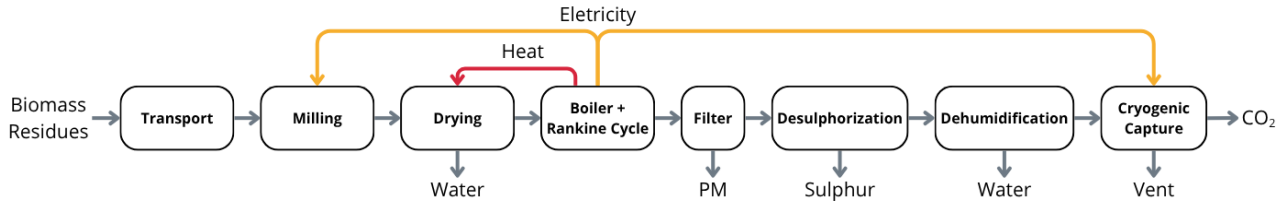

Figure 1. *Forest-residues-fuelled Rankine-based plant with cryogenic CO_2 capture process diagram.*

Biomass combustion was modelled using an overall stoichiometric reaction based on the elemental composition of the fuel reported in Table 2. The biomass was represented by an empirical formula derived from its ultimate analysis (C, H, O, S), and complete combustion with excess air was assumed. The global combustion reaction was modelled as expressed in Eq. (1).

$$C_x H_y O_z S_w + \left(x + \frac{y}{4} - \frac{z}{2} + w\right) O_2 \rightarrow x\, CO_2 + \frac{y}{2} H_2O + w\, SO_2 \quad (1)$$

where the coefficients are determined from elemental composition. The model assumes complete conversion of carbon to CO_2, hydrogen to H_2O, and sulphur to SO_2, while nitrogen is treated as inert. Ash is separated into bottom ash and fly ash fractions converted directly from mass input to the boiler on a dry basis.

The energy released during combustion is calculated based on the Low Heating Value (LHV) of the biomass, and boiler efficiency is applied to determine the useful heat available for process integration and power generation.

The LHV of the biomass is fixed at 18 MJ/kg (db), and no seasonal or compositional variability is considered. Ash generated during combustion is assumed to be inert and is partitioned into bottom ash and fly ash fractions, which are handled separately in the process model. Biomass supply is assumed to be continuous and homogeneous, and no preprocessing beyond grinding and drying is considered.

Table 2*. Biomass properties and composition assumptions.*

Data	Value	Units / db	Ref.
Moisture	45	% / wb	[18]
Ash	2	%	
C	50	%	
H	7	%	
O	42.6	%	
S	0.4	%	
LHV	18	MJ/kg	
ρ	0.2	t/m^3	

2.2. Techno-Economic Assessment

Plant-level capital expenditure was obtained by aggregating itemized equipment costs, adapting methodologies previously used [19 - 21]. For each process unit, Purchased Equipment Cost (PEC) in euros was estimated from sizing correlations following Eq. (2).

$$PEC_i = C_{0,i} \times \left(\frac{S_i}{S_{0,i}}\right)^n \times \left(\frac{CEPCI_{\text{now}}}{CEPCI_{\text{ref}}}\right), \quad i = Equipments \quad (2)$$

where $C_{0,i}$ is the reference cost at reference size $S_{0,i}$ and reference year, $S_i$is the current size, n is the scaling factor, and the last ratio corrects costs using the Chemical Engineering Plant Cost Index (CEPCI) from the reference year to the current one. The PEC equations considered for each equipment are shown in Table 3.

Each equation was obtained either directly from the source or derived based on the equipment's source type, capacity, and cost.

***Table 3**. Equipment cost correlations and sizing variables used for CAPEX estimation.*

Equipment	Eq. Year	Sizing Variable (S)	Cost Equation* / $M€$	Ref.
Grinder	2017	Feed wb (t/d)	$PEC = 0.153 \times \left(\frac{S}{2140}\right)^{1.00}$	
Dryer	2017	Output db (t/d)	$PEC = 0.321 \times \left(\frac{S}{1100}\right)^{0.70}$	[21]
Boiler	1994	Air inlet (kg/s) and furnace temperature (K)	$PEC = 0.00004608 \times \frac{S_{\text{air}}}{0.995 - 0.98} \times (1 + e^{0.018 S_T - 26.3})$	[22]
Turbine	2021	Installed Power (kW)	$PEC = 0.00516 \times S^{0.7}$	[23]
Filter	2012	Volumetric input (m^3/s)	$PEC = 0.0791 \times \left(\frac{S}{15.6}\right)^{0.70}$	[24]
Desulphurization unit	2008	Sulphur flow rate (t/h)	$PEC = 37.32 \times \left(\frac{S}{2.4}\right)^{0.80}$	[25]
Dehumidification unit	2010	Volumetric input (m^3/h)	$PEC = 0.0734 \times \left(\frac{S}{7000}\right)^{0.70}$	[24]
Cryogenic Unit	2023	CO_2 Feed (kg/s)	$PEC = 4.69 \times \left(\frac{S}{1.087}\right)^{0.80}$	[11]

The Total Capital Investment (TCI) in euros is obtained by applying a factor accounting for direct costs, indirect costs and working capital assumed equal to every equipment considered according to Eq. (3).

$$TCI = \left(\sum_{i=1}^{N} P\,EC_i\right) \times F_{\text{TCI}} \tag{3}$$

Where the aggregated factor F_{TCI},

$$F_{TCI} = \overbrace{\left(1+f_{\text{inst}}+f_{\text{pipe}}+f_{\text{elec}}+f_{\text{civil}}\right)}^{Direct\ Costs} \times \overbrace{\left((1+f_{\text{EPCM}}) \times (1+f_{\text{cont}}+f_{\text{owner}})\right)}^{Indirect\ Costs} \times \overbrace{\left(1+f_{\text{working}}\right)}^{Working\ Capital} \tag{4}$$

Where f_{inst}, f_{pipe}, f_{elec}, and $f_{\text{civil}}$are the installation, piping, electrical, and civil works cost factors, respectively, which together represent installation-related direct costs applied to the purchased equipment cost. f_{EPCM}, f_{cont}, and f_{owner} are the Engineering, Procurement and Construction Management (EPCM), contingency, and owner's cost factors, respectively, which together represent indirect costs. $f_{\text{working}}$is the working capital factor applied to finally achieve the Total Capital Investment (TCI). The values assumed for the referred factors are in Table 4.

***Table 4**. Considered fractions for CAPEX assessment.*

Factor	f_{inst}	f_{pipe}	f_{elec}	f_{civil}	f_{EPCM}	f_{cont}	f_{owner}	f_{working}
Value	0.1	0.4	0.2	0.13	0.20	0.20	0.15	0.1
Ref.		[26]				[27]		[28]

Operating expenditure (OPEX) was calculated on an annual basis and decomposed into variable (throughput-dependent) and fixed (capacity-dependent) components. Variable OPEX includes feedstock, utilities, and consumables, and was computed from process simulation outputs and corresponding unit prices. Fixed OPEX includes operation and maintenance, labor, and overhead costs, which were estimated as fractions of total capital investment or as annualized costs independent of throughput. The total annual operating cost in euros is given by Eq. (5).

$$OPEX = \frac{\overbrace{C_{\text{raw}} + C_{\text{elec}}}^{Variable\ OPEX} + \overbrace{C_{\text{over}} + C_{\text{O\&M}}}^{Fixed\ OPEX}}{(1 - f_{\text{sell}} - f_{\text{admin}})} \tag{5}$$

where C_{raw}, C_{elect} represent the variable operating cost components, namely raw material costs and electricity cost, respectively. $C_{\text{raw}} = C_{\text{biomass}} + C_{\text{transport}} + C_{\text{ash}}$ includes biomass purchase and transportation costs, and ash disposal. Biomass transportation cost is estimated based on truck payload, number of trips, and fixed

distance-dependent costs. C_{over} and $C_{\text{O\&M}}$ represent fixed operating costs, with C_{over} denoting plant overhead and $C_{\text{O\&M}} = C_{\text{labor}} + C_{\text{clerical}} + C_{\text{rep}} + C_{\text{sup}} + C_{\text{lab}}$ including labor, clerical, maintenance, supplies, and laboratory costs. Finally, f_{sell} and f_{admin} are the selling and administrative cost fractions applied to the net operating expenditure. Process parameters assumed for OPEX calculations are shown in Table 5.

***Table 5**. Variable and fixed OPEX assumptions.*

Parameter	Value	Unit	Ref.
Variable OPEX			
Biomass	50	€/t	[29]
Biomass transportation	2.5	€/km	[30]
Electricity	75	€/MWh	[31]
Ash disposal	18	€/t	[25]
Boiler Efficiency	85	%	[24]
Steam to Power Efficiency	17	%	[20]
Specific Energy Consumption (SEC)			
Grinder	25	kWh/t of feed wb	[32]
Drier	734	kWh/t of dried product	[24]
Bag filter	0.0003	kWh/kg of feed	[33]
Dehumidifier	0.70	kWh/kg of condensed water	[34]
Desulphurization Unit	0.05	kWh/kg of feed wb	[17]
Cryogenic Capture Unit	409.7	kWh/t_{CO_2}	Tuned based on [4 - 6], [11 - 15]
Fixed OPEX			
Repairs	1	% of TCI	[28]
Supplies	0.2	% of TCI	
Administrative	2.5	% of TCI	
Selling	3	% of TCI	
Employee number			[25]
50 kt/y input	28	-	
100 kt/y input	35	-	
200 kt/y input	42	-	
500 kt/y input	56	-	
Employee average salary	36 000	€/y	[29]
Clerical	15	% of Labor Costs	[28]
Lab charge	15	% of Labor Costs	
Overheads	35	% of Labor Costs	

The Carbon Capture Cost (CCC) was evaluated to quantify the economic effort required to deliver purified biogenic CO_2 from forest residues according to Eq. (6). The CCC in $€/t_{CO_2}$ was defined at the system level, encompassing all process units from biomass pre-treatment and combustion to flue gas cleaning and cryogenic CO_2 capture.

$$CCC = \frac{OPEX + \left[(1 - f_{\text{salv}}) \times TCI \times \left(\frac{r(1+r)^N}{(1+r)^N - 1}\right)\right]}{M_{co_2}} \quad (6)$$

Where r is the interest rate, N is the plant lifetime, f_{salv} is the salvage factor and M_{co_2} is the annual mass of CO_2 captured in t/y. Financial assumptions for CCC calculations are shown in Table 6.

***Table 6**. Financial assumptions considered for the economic assessment.*

Parameter	N	Operating Hours	r	f_{salv}
Value	25	8000	5	4
Unit	y	h/y	%	%
Ref.	[35]		[29]	[36]

2.2.1. Sensitivity Analysis

A local sensitivity analysis was performed to evaluate the impact of key technical and economic parameters on the carbon capture cost (CCC). Each parameter was independently varied by ± 20 % relative to its baseline value, while keeping all other variables constant (one-at-a-time approach).

Two groups of parameters were analysed:

- Technical parameters: biomass moisture content, boiler efficiency, and SEC of major process units (CO_2 capture, dehumidification, drying, milling, desulphurization, and bag filter);

- Economic parameters: Annualized Capital Expenditure (CAPEX), OPEX components (biomass cost, transportation cost, electricity cost), plant lifetime, and interest rate.

The analysis was conducted for all four plant capacities (50, 100, 200, and 500 kt/y) to assess scale-dependent effects. The resulting variation in CCC was expressed as a percentage change relative to the base case.

3. Results and Discussion

3.1. Mass and Energy Balances

The mass balance results for the 200 kt/y case are shown in Table 7. It was possible to capture CO_2 in the solid state at a rate of 6.384 kg/s. For the 50, 100, and 500 kt/y biomass input masses, it was possible to recover 1.68, 3.36, and 16.80 kg/s of solid CO_2, respectively.

Biomass input decreases from 6.944 to 6.806 kg/s in the milling unit as a fixed 2% of mass loss is assumed. In the dryer, mass reduction is solely attributed to water removal, with no solids drag considered. Water decreases from 3.062 kg/s to 0.416 kg/s, corresponding to an 86% removal, reflecting a reduction in biomass moisture from 45% to 10%.

In the boiler, the total mass flow increases to 31.857 kg/s due to air addition (27.698 kg/s) under 20% excess air conditions. Complete conversion of biomass is assumed according to Eq. (1), with no NO_x formation. The flue gas is composed mainly of N_2 (21.247 kg/s), CO_2 (6.720 kg/s), H_2O (2.710) and unreacted O_2 (1.075 kg/s). Ash production is fixed at 2 wt% of dry biomass inlet, split into bottom ash (0.052 kg/s) and fly ash (0.022 kg/s).

Gas cleaning units primarily perform separations and conditioning for CO_2 cryogenic capture. Bottom ashes are completely removed within the boiler, while the bag filter removes 99% of the fly ash, reducing its flow to 0.0002 kg/s. The desulphurization is set to 97% following [25], decreasing SO_2 emissions from 0.029 to 0.001 kg/s. The dehumidifier condenses 90% of water (2.710 to 0.271 kg/s). Finally, the CO_2 capture unit recovers 6.384 kg/s from 6.720 kg/s, reflecting the fixed 95% capture efficiency. The remaining components are assumed to be fully separated from the CO_2 in the cryogenic system.

***Table 7**. Mass balance results of main streams/equipments across process units for the 200 kt/y case.*

Component, kg/s	Dryer		Boiler		Bag filter		Desulphurization		Dehumidifier		CO_2 capture	
	In	Out	In	Out	In	Out	In	Out	In	Out	In	Out
Total mass flow*	6.806	4.159	31.857	31.857	31.804	31.782	31.782	31.754	31.754	29.314	29.314	29.314
Air	0	0	27.698	0	0	0	0	0	0	0	0	0
Biomass	3.743	3.743	3.743	0	0	0	0	0	0	0	0	0
H_2O	3.062	0.416	0.416	2.710	2.710	2.710	2.710	2.710	2.710	0.271	0.271	0
CO_2	0	0	0	6.720	6.720	6.720	6.720	6.720	6.720	6.720	6.720	6.384
N_2	0	0	0	21.247	21.247	21.247	21.247	21.247	21.247	21.247	21.247	0
O_2	0	0	0	1.075	1.075	1.075	1.075	1.075	1.075	1.075	1.075	0
SO_2	0	0	0	0.029	0.029	0.029	0.029	0.001	0.001	0.001	0.001	0
Bottom	0	0	0	0.052	0	0	0	0	0	0	0	0
Fly ash	0	0	0	0.022	0.022	0.0002	0.0002	0.0002	0.0002	0.0002	0.0002	0

*Discrepancies between inlet and outlet total mass flows in some units arise from the exclusion of secondary streams.

The overall energy balance is governed by the assumed unit efficiencies and SEC values summarized in Table 5. Biomass combustion provides the primary energy input, with the boiler efficiency limited to 85% [24], accounting for flue gas sensible heat losses between furnace temperature (800 ºC) and stack conditions (160 ºC). These losses were estimated using flue gas composition with constant heat capacities. Although a theoretical efficiency of 93% is obtained considering only stack losses, additional unmodelled losses justify the lower implemented value. This heat, carried by the flue gas, is used to offset part of the drying demand in a waste energy recovery approach.

Electricity generation via the Rankine cycle is calculated by the heat-to-power efficiency of 17% adopted from [20], which determines the fraction of useful thermal energy converted into electricity. It should be noted that the biomass thermal input reported in Table 8 is based on the process feed. Therefore, the effective boiler input is slightly reduced by preprocessing losses (e.g., 2% in milling).

The distribution of energy demand across unit operations reflects the adopted SEC values. Grinding (25 kWh/t) remains a minor contributor, while drying (734 kWh/t) represents the only thermal sink. However, the electrical demand is dominated by gas treatment steps, particularly the dehumidifier (0.70 kWh/kg of condensed water) and the cryogenic CO_2 capture unit (409.7 kWh/t_{CO_2}), which together account for 93.2% of all process electrical

demand (Table 8). Considering the whole process electric demand without integration of boiler electricity, the gross process specific energy for CO_2 capture is 726.5 against the net 363.1 kWh/t_{CO_2}, considering the integration of the electricity produced from boiler steam. This demonstrates that the net energy penalty is strongly influenced by the balance between electricity generation and consumption, highlighting the importance of efficient heat-to-power conversion and process integration.

The biomass combustion provides sufficient heat for offsetting the drying step and enables net power generation (e.g., 2.1 – 29.1 MWe across scales). However, this is offset by the high electricity requirements of CO_2 capture and flue gas conditioning. Therefore, the energy penalty is dominated by the capture step rather than biomass conversion, highlighting that process improvements should focus on reducing capture energy intensity and enhancing heat integration and heat-to-power integration while maximizing boiler and electricity production efficiencies.

***Table 8**. Equipment installed capacity for each case.*

Installed Capacity, MWe	Biomass Input, kt/y			
	50	100	200	500
Biomass Input Thermal Power (MWth)	17.2	34.4	68.8	171.9
Boiler Useful Thermal Power (MWth)	14.0	28.1	56.1	140.3
Dryer Thermal Power Needs (MWth)	1.8	3.5	7.0	17.5
Boiler Electricity Generation	2.1	4.2	8.4	20.9
Grinder	0.16	0.31	0.63	1.56
Bag Filter	0.008	0.016	0.032	0.08
Desulphurization	0.12	0.24	0.48	1.19
Dehumidifier	1.54	3.07	6.15	15.37
CO_2 Capture	2.35	4.71	9.42	23.54

3.2. Techno-Economic Assessment

The techno-economic assumptions presented in Table 3 – 6 established the methodological backbone for the cost distributions and trends observed in Figure 2 – 5. The adopted cost correlations follow a standard power-law formulation (Eq. (2)), in which the PEC scales with capacity through an exponent n, reflecting the degree of economies of scale. This formulation is consistent with established methodologies in techno-economic systems modelling, where capital cost behaviour is strongly governed by scaling laws derived from reference plant data.

A key aspect of the selected correlations is the variation of the scaling exponent n across different equipment. Units such as the grinder exhibit an exponent close to unity, indicating near-linear scaling and therefore negligible economies of scale (i.e. modular equipment). In contrast, most thermochemical and separation units, such as the dryer, filter, dehumidification unit, desulphurization units, and the cryogenic CO_2 capture unit, present sub-linear exponents (typically 0.7 – 0.8). This implies that costs increase at a slower rate than capacity, leading to a reduction in specific investment cost as plant size increases. This effect directly explains the decreasing contribution of CAPEX per unit of CO_2 captured observed in Figure 2, where larger plants (e.g., 500 kt/y) benefit disproportionately from scale compared to smaller configurations.

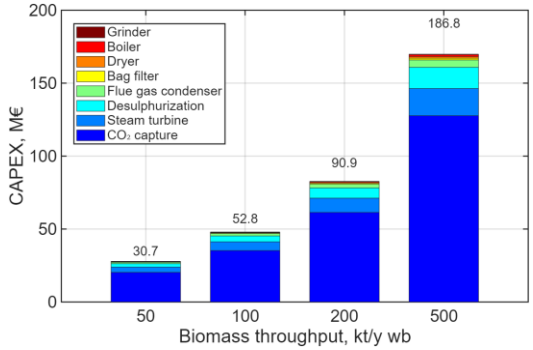

***Figure 2**. CAPEX breakdown by equipment.*

The influence of the scaling exponent becomes particularly relevant when interpreting the relative contribution of different units to total CAPEX. Equipment with both high base cost and low scaling exponent (such as the cryogenic CO_2 capture unit) tends to dominate the investment at small scale but becomes relatively less penalizing at larger capacities. This behaviour is reflected in Figure 2, where the capture unit remains a major

contributor across all cases but shows a reduced relative weight as plant size increases. This trend is consistent with literature on cryogenic systems [4 - 16], which highlights both their high initial capital intensity and their improved competitiveness at larger scales due to favorable scaling behaviour.

The aggregation of PEC into TCI through the fractional factors in Table 6 further amplifies these scaling effects. The inclusion of installation, piping, electrical, civil works, EPCM, contingency, and owner's costs results in a multiplicative expansion of the PEC. Because these factors are applied proportionally, any reduction in PEC driven by scaling exponents is propagated to the total CAPEX. Consequently, the economies of scale embedded in Eq. (2) are not only preserved but magnified at the plant level, reinforcing the strong CAPEX reduction trends observed in the results.

On the operational side, the structure presented in Table 5 introduces a combination of variable and fixed costs that interact differently with plant capacity. Variable costs (particularly biomass acquisition and transportation, and electricity purchase) scale directly with throughput, while fixed costs are partially linked to CAPEX or labor assumptions. The dominance of electricity costs, especially those associated with the cryogenic CO_2 capture unit and gas conditioning steps, is consistent with the energy balance results and explains the trends observed in Figures 3 and 4. As shown in the process analysis, the capture unit alone accounts for a substantial fraction of total electrical demand, which translates directly into OPEX due to the assumed electricity price. This is in line with reported behaviour of cryogenic capture systems [6 - 8], [11], [13], where operational costs are highly sensitive to energy consumption.

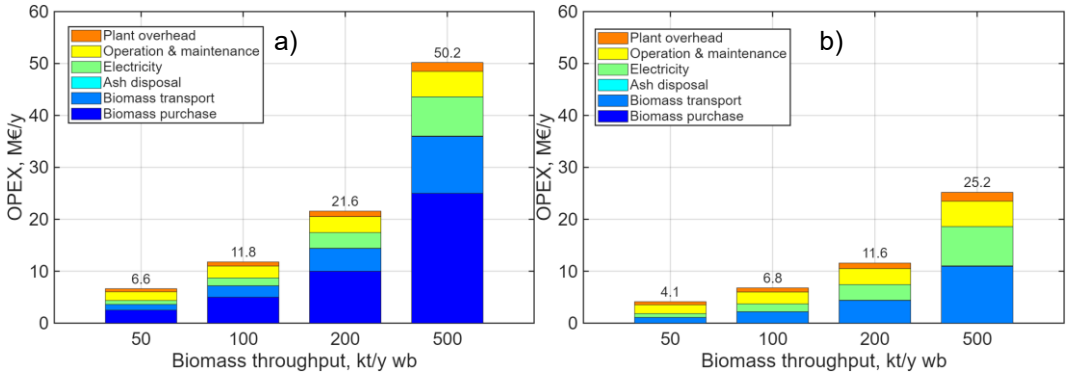

***Figure 3**. OPEX breakdown by cost component for a) 50€/t of biomass and b) zero biomass purchase cost.*

As observed in Figure 3, biomass purchase and transportation are the dominant costs in operational expenditures, particularly when electricity demand is partially offset by internal generation from the process power generation unit. This highlights the importance of boiler and Rankine cycle efficiencies, which may lead to an energy autonomous process if coupled with more energy-efficient gas conditioning and cryogenic system. However, biomass especially forest residues, may be obtained at zero cost. Considering this scenario, the OPEX would be reduced by 37, 42, 45, and 49 % for 50, 100, 200, and 500 kt/y cases, respectively. This would, therefore, lead to a CCC reduction of 28, 32, 35, and 39 % for 50, 100, 200, and 500 kt/y cases, respectively as shown in Figure 5.

While CAPEX benefits from economies of scale through the exponent n, OPEX does not exhibit the same degree of reduction. Biomass costs and transport costs remain largely proportional to plant capacity, meaning that their contribution to total OPEX remains significant across all scales. This clarifies why, in Figure 3, feedstock-related costs maintain a dominant share even at higher capacities. Therefore, the limited scaling of OPEX compared to CAPEX ultimately leads to a diminishing but non-negligible reduction in CCC with increasing plant size, as shown in Figure 5.

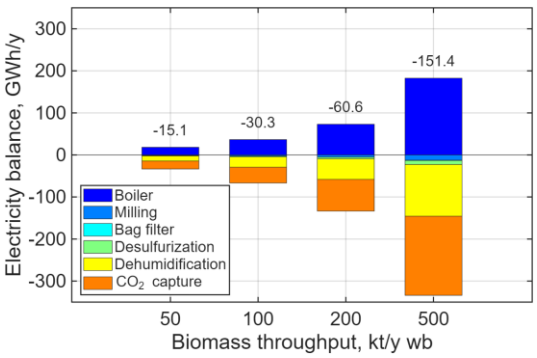

***Figure 4**. Electricity balance by process unit. Negative values indicate electricity purchase from the grid.*

The financial assumptions in Table 6 further influence the translation of CAPEX and OPEX into CCC. The relatively long plant lifetime (25 years) and moderate discount rate (5%) allow capital costs to be distributed over extended operation, enhancing the impact of CAPEX reductions achieved through scaling. As a result, the benefits of lower scaling exponents are more pronounced in the levelized metrics, reinforcing the observed decrease in CCC with plant size (Figure 5).

Overall, the combination of power-law cost correlations, cost factorization, and operational assumptions creates a coherent framework. The results demonstrate that while economies of scale significantly reduce CAPEX-driven costs, the overall system remains constrained by energy-intensive CO_2 capture and feedstock-related OPEX. This interplay explains the trends observed across figures and highlights that further cost reductions are likely to depend not only on scaling but also on improvements in energy efficiency and process integration, particularly within the capture section.

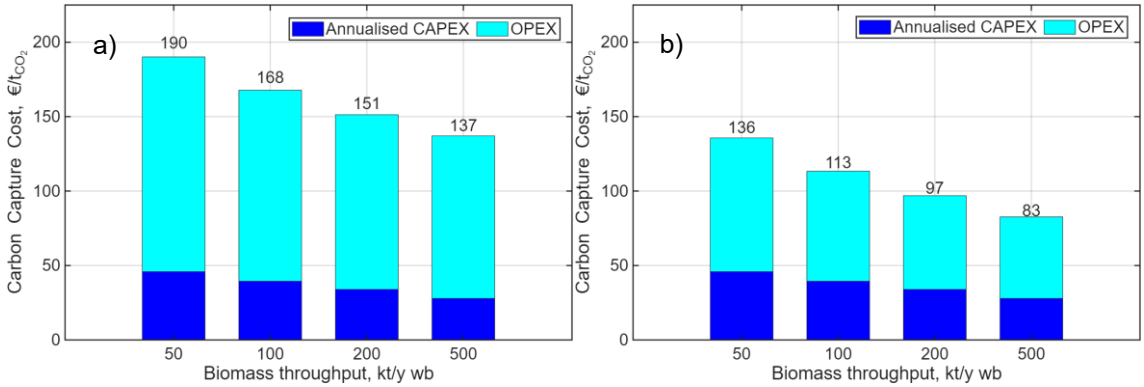

***Figure 5**. Carbon capture cost breakdown a) with and b) without biomass purchase cost.*

3.3. Sensitivity Analysis

The sensitivity analysis results presented in Figure 6a highlight the dominant influence of technical parameters on the CCC. Biomass moisture content emerges as the most influential variable, showing the highest variation in CCC (up to 10 – 11 %). Unlike unit-specific SEC parameters, the biomass moisture simultaneously affects dryer duty, wet-basis fuel heating value, internal electricity generation, and the amount of dry biomass converted to CO_2, thereby altering both the annualized system cost and the captured-CO_2 denominator used in the CCC calculation. However, a slight asymmetry is observed, with moisture reduction (−20 %) leading to a marginally stronger decrease in CCC compared to the increase caused by higher moisture (+20 %). This indicates that improvements in feedstock quality provide slightly greater economic benefits than the penalties associated with more humid biomass. As a result, higher moisture contents penalize both energy efficiency and operational costs, confirming that feedstock quality is a critical parameter in biomass-based systems. Similarly, boiler efficiency and heat-to-power efficiency (HTP efficiency) exhibit a significant impact, with variations in CCC reaching 1 – 3 %. These parameters govern the balance between internally generated electricity and external electricity demand, reinforcing the importance of efficient energy conversion and integration within the system.

The second most influential parameter is the SEC of the CO_2 capture unit due to its high electric consumption, with changes leading to CCC variations of 2 – 3 %. This is consistent with the energy balance discussion, where the cryogenic capture unit represents the largest share of electricity demand. Variations in dehumidification SEC show a comparable but slightly lower influence, reflecting its role as a key upstream conditioning step that directly affects the thermal and electrical load of the cryogenic system. In contrast, the SEC of auxiliary units such as drying (on a per-unit basis), milling, desulphurization, and bag filtration exhibits a negligible effect on CCC. This indicates that, although these units are necessary for process operation, their relative contribution to the overall energy penalty is minor.

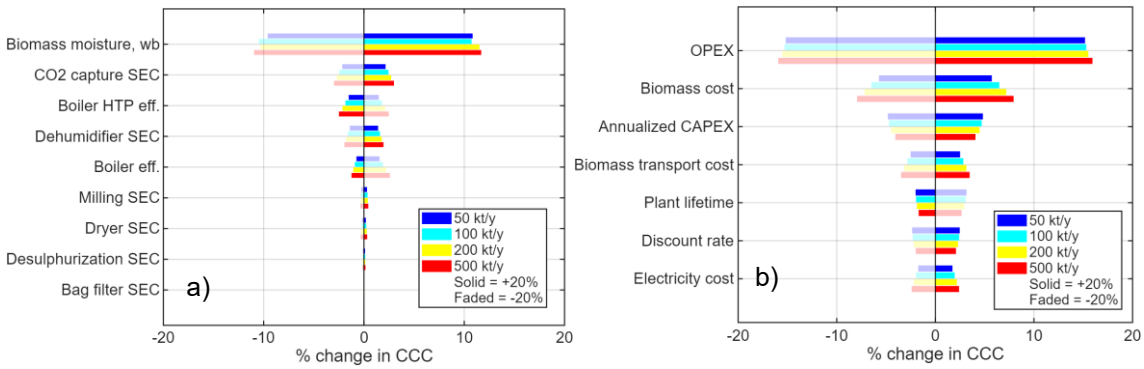

***Figure 6**. Sensitivity of carbon capture cost on a) technical parameters and b) economic parameters.*

Figure 6b presents the sensitivity to economic parameters and further reveals the cost structure of the system. OPEX shows the highest impact on CCC, with variations reaching ± 15 %, confirming that the system is predominantly OPEX-driven. Within OPEX, biomass cost is the most influential component, leading to CCC variations of about ± 6 – 8 %, followed by annualized CAPEX, which contributes approximately ± 4 – 5 %. Biomass transportation cost shows a slightly lower but still relevant impact, with variations around ± 3 – 4 %. These results are consistent with the OPEX breakdown discussed previously, where feedstock-related costs dominate across all scales due to their direct proportionality with throughput. The relatively stronger influence of annualized CAPEX compared to transportation costs reflects the contribution of capital-related charges to total cost formation, particularly at smaller scales where specific investment costs are higher.

Financial parameters such as plant lifetime and discount rate show a comparatively lower effect, within 1 – 2 %, indicating that the economic performance is less sensitive to financing assumptions than to operational costs. However, it is noteworthy that their relative influence is more pronounced in smaller-scale plants, which contrasts with the general trend observed for most technical and economic parameters. This behaviour can be explained by the higher specific CAPEX (€/tCO_2) associated with smaller installations, resulting from limited economies of scale embedded in the cost correlations. Therefore, annualized CAPEX represents a larger fraction of the total CCC at small scale, making it more sensitive to financial assumptions such as discount rate and plant lifetime. In larger plants, the reduction in specific CAPEX dilutes the contribution of capital-related costs, thereby decreasing the sensitivity to these parameters.

Electricity cost, despite being a key contributor to OPEX, shows a limited sensitivity. This is explained by the partial energy self-sufficiency of the system through cogeneration, which mitigates the impact of external electricity price fluctuations. Across most other parameters, larger plants tend to exhibit reduced sensitivity due to economies of scale and improved energy integration. In contrast, the inverse trend observed for financial parameters reinforces that capital cost structure plays a disproportionately important role at smaller scales, where CAPEX dominates over OPEX in the overall cost formation.

4. Conclusion

This work presented a comprehensive techno-economic assessment of a forest-residues-based electric generation system integrated with cryogenic CO_2 capture via anti-sublimation, addressing a key gap in the evaluation of decentralized biomass-based low-neutral emission technologies. The results demonstrate that, although the system benefits from economies of scale, reducing specific CAPEX and carbon capture cost (CCC) with increasing plant capacity, the overall performance remains strongly constrained by operational factors. In particular, the process is predominantly OPEX-driven, with biomass supply and transportation costs representing the largest contributors, while the cryogenic capture and dehumidification unit dominates the energy demand, accounting for over 90% of electricity consumption. The integration of internal electricity generation significantly reduces the effective energy penalty, yet the specific energy consumption of the capture unit remains a critical bottleneck. Sensitivity analysis confirmed that technical parameters such as biomass moisture content, boiler efficiency, and capture SEC have the highest impact on CCC, whereas financial parameters exhibit comparatively minor influence, particularly at larger scales. The findings highlight that future improvements should prioritize reducing energy intensity in the capture section, enhancing heat and power integration, and optimizing biomass logistics and feedstock quality. Overall, the study supports the feasibility of decentralized BECCS configurations based on forest residues, while emphasizing that cost competitiveness will depend on simultaneous advances in process efficiency and supply chain optimization.

Acknowledgements

João Roberto F. S. acknowledges FCT, the Portuguese Foundation for Science and Technology, for the PhD grant no. 2024.06283.BD and the Transmit COST Action (CA21127 - Techno-economic analysis of carbon

mitigation technologies (TrANsMIT)) for the support under the Young Researcher and Innovator Conference grant. This research was funded by the European Regional Development Fund of the European Union through the Innovation and Digital Transition Program (COMPETE 2030) of Portugal 2030 under the project Bio-Waste2Carbon (BW2C): Cryogenic carbon capture of post-combustion gases from forestry residues, contract number COMPETE2030-FEDER-00591900. This work was also funded in part by the Fundação para a Ciência e a Tecnologia, I.P. (FCT) under the multiannual funding program UID/50022/2025 (DOI: 702 10.54499/UID/50022/2025). The researchers from CERES acknowledge FCT (Fundação para a Ciência e a Tecnologia, Portugal) and the European Regional Development Fund for the financial support of projects with DOI https://doi.org/10.54499/UID/00102/2025, https://doi.org/10.54499/UID/PRR/00102/2025 and https://doi.org/10.54499/UID/PRR2/00102/2025.

References

[1] Intergovernmental Panel on Climate Change (IPCC), *Climate Change 2022: Mitigation of Climate Change*. Cambridge, United Kingdom and New York, NY, USA: Cambridge University Press, 2022. doi: 10.1017/9781009157926.

[2] International Energy Agency (IEA), 'CCUS in Clean Energy Transitions', International Energy Agency, Paris, France, 2020. [Online]. Available: https://www.iea.org/reports/ccus-in-clean-energy-transitions

[3] F. S. João Roberto, J. B. Ribeiro, and L. Durães, 'e-Fuel production process technologies and trends: A bibliometric-based review', *Energy Reports*, vol. 13, pp. 3351–3368, Jun. 2025, doi: 10.1016/j.egyr.2025.02.030.

[4] A. A. Alsanousie, A. E. Attia, M. Elhelw, and O. A. Elsamni, 'Towards nearly zero emissions natural gas-fired power plants using cryogenic carbon dioxide capture technology', *International Journal of Greenhouse Gas Control*, vol. 127, p. 103928, Jul. 2023, doi: 10.1016/j.ijggc.2023.103928.

[5] R. Sun *et al.*, 'Performance analysis and comparison of cryogenic CO_2 capture system', *International Journal of Green Energy*, vol. 18, no. 8, pp. 822–833, Jun. 2021, doi: 10.1080/15435075.2021.1880916.

[6] M. J. Tuinier, H. P. Hamers, and M. Van Sint Annaland, 'Techno-economic evaluation of cryogenic CO2 capture—A comparison with absorption and membrane technology', *International Journal of Greenhouse Gas Control*, vol. 5, no. 6, pp. 1559–1565, Nov. 2011, doi: 10.1016/j.ijggc.2011.08.013.

[7] C. Kolster, E. Mechleri, S. Krevor, and N. Mac Dowell, 'The role of CO 2 purification and transport networks in carbon capture and storage cost reduction', *International Journal of Greenhouse Gas Control*, vol. 58, pp. 127–141, Mar. 2017, doi: 10.1016/j.ijggc.2017.01.014.

[8] A. Costa, D. Coppitters, L. Dubois, F. Contino, D. Thomas, and G. De Weireld, 'Energy, exergy, economic and environmental (4E) analysis of a cryogenic carbon purification unit with membrane for oxyfuel cement plant flue gas', *Applied Energy*, vol. 357, p. 122431, Mar. 2024, doi: 10.1016/j.apenergy.2023.122431.

[9] H. Li, Y. Hu, M. Ditaranto, D. Willson, and J. Yan, 'Optimization of Cryogenic CO2 Purification for Oxy-coal Combustion', *Energy Procedia*, vol. 37, pp. 1341–1347, 2013, doi: 10.1016/j.egypro.2013.06.009.

[10] Z. Wu, G. Xu, W. Zhang, X. Xue, and H. Chen, 'Thermodynamic and economic analysis of a new methanol steam reforming system integrated with CO2 heat pump and cryogenic separation system', *Energy*, vol. 283, p. 128501, Nov. 2023, doi: 10.1016/j.energy.2023.128501.

[11] H. Asgharian *et al.*, 'Techno-economic analysis of blue ammonia synthesis using cryogenic CO2 capture Process-A Danish case investigation', *International Journal of Hydrogen Energy*, vol. 69, pp. 608–618, Jun. 2024, doi: 10.1016/j.ijhydene.2024.05.060.

[12] D. K. De, I. A. Oduniyi, A. A. Sam, A. M. Aneesh, and S. Akinmeji, 'Modelling carbon capture from power plants with low energy and water consumption using a novel cryogenic technology', *Applied Thermal Engineering*, vol. 257, p. 124315, Dec. 2024, doi: 10.1016/j.applthermaleng.2024.124315.

[13] W. Noh, S. Park, Y. Kim, J. Lee, J. Kim, and I. Lee, 'Systems design and techno-economic analysis of a novel cryogenic carbon capture process integrated with an air separation unit for autothermal reforming blue hydrogen production system', *Journal of Cleaner Production*, vol. 457, p. 142341, Jun. 2024, doi: 10.1016/j.jclepro.2024.142341.

[14] C. E. Swanson, J. W. Elzey, R. E. Hershberger, R. J. Donnelly, and J. Pfotenhauer, 'Thermodynamic analysis of low-temperature carbon dioxide and sulfur dioxide capture from coal-burning power plants', *Phys. Rev. E*, vol. 86, no. 1, p. 016103, Jul. 2012, doi: 10.1103/PhysRevE.86.016103.

[15] M. J. Tuinier, M. Van Sint Annaland, and J. A. M. Kuipers, 'A novel process for cryogenic CO2 capture using dynamically operated packed beds—An experimental and numerical study', *International Journal of Greenhouse Gas Control*, vol. 5, no. 4, pp. 694–701, Jul. 2011, doi: 10.1016/j.ijggc.2010.11.011.

[16] M. M. Shah, 'Carbon dioxide (CO 2) compression and purification technology for oxy-fuel combustion', in *Oxy-Fuel Combustion for Power Generation and Carbon Dioxide (CO2) Capture*, Elsevier, 2011, pp. 228–255. doi: 10.1533/9780857090980.2.228.

[17] G. Qiu, H. Wei, X. Liang, Z. Li, F. Wang, and Y. Zhu, 'Energy Consumption Analysis of Desulphurization Ultra-low Emission Operation and Outlook on Its Energy-saving Operation in Thermal Power Plants', *Power Generation Technology*, vol. 41, no. 5, pp. 509–516, 2020, doi: 10.12096/j.2096-4528.pgt.20040.
[18] A. Pires, E. Cancela, N. Alves, T. Almeida, S. Figo, and L. Gil, 'Variability and quality profiles of solid biofuels from standardized laboratory analyses', *Academia Green Energy*, vol. 2, no. 4, Dec. 2025, doi: 10.20935/AcadEnergy8031.
[19] M. Al-Breiki and Y. Bicer, 'Techno-economic evaluation of a power-to-methane plant : Levelized cost of methane, financial performance metrics, and sensitivity analysis', *Chemical Engineering Journal*, vol. 471, p. 144725, Sep. 2023, doi: 10.1016/j.cej.2023.144725.
[20] A.-M. Cormos and C.-C. Cormos, 'Techno-economic assessment of combined hydrogen & power co-generation with carbon capture: The case of coal gasification', *Applied Thermal Engineering*, vol. 147, pp. 29–39, Jan. 2019, doi: 10.1016/j.applthermaleng.2018.10.064.
[21] A. Singlitico, I. Kilgallon, J. Goggins, and R. F. D. Monaghan, 'GIS-based techno-economic optimisation of a regional supply chain for large-scale deployment of bio-SNG in a natural gas network', *Applied Energy*, vol. 250, pp. 1036–1052, Sep. 2019, doi: 10.1016/j.apenergy.2019.05.026.
[22] E. Açıkkalp, R. Zairov, and D. Borge-Diez, 'Biomass-based electricity, methanol and hydrogen production with CO2 and carbon co-electrolysis: Energy, exergy, economic and sustainability analyses', *Renewable Energy*, vol. 256, p. 124492, Jan. 2026, doi: 10.1016/j.renene.2025.124492.
[23] W. Wu, M. I. Taipabu, W.-C. Chang, K. Viswanathan, Y.-L. Xie, and P.-C. Kuo, 'Economic dispatch of torrefied biomass polygeneration systems considering power/SNG grid demands', *Renewable Energy*, vol. 196, pp. 707–719, Aug. 2022, doi: 10.1016/j.renene.2022.07.007.
[24] J. M. Ahlström, K. Pettersson, E. Wetterlund, and S. Harvey, 'Value chains for integrated production of liquefied bio-SNG at sawmill sites – Techno-economic and carbon footprint evaluation', *Applied Energy*, vol. 206, pp. 1590–1608, Nov. 2017, doi: 10.1016/j.apenergy.2017.09.104.
[25] C.-C. Cormos *et al.*, 'Synthetic natural gas (SNG) production by biomass gasification with CO2 capture: Techno-economic and life cycle analysis (LCA)', *Energy*, vol. 312, p. 133507, Dec. 2024, doi: 10.1016/j.energy.2024.133507.
[26] J. Witte, A. Kunz, S. M. A. Biollaz, and T. J. Schildhauer, 'Direct catalytic methanation of biogas – Part II: Techno-economic process assessment and feasibility reflections', *Energy Conversion and Management*, vol. 178, pp. 26–43, Dec. 2018, doi: 10.1016/j.enconman.2018.09.079.
[27] E. Giglio, M. Bianco, G. Zanardi, E. Catizzone, G. Giordano, and M. Migliori, 'Direct biogas methanation via renewable-based Power-to-Gas: Techno-economic assessment based on real industrial data', *Energy Conversion and Management*, vol. 332, p. 119775, May 2025, doi: 10.1016/j.enconman.2025.119775.
[28] X. Liu, T. K. Poddar, J. Zhang, X. Su, T. R. Hawkins, and H. Huang, 'Techno-economic analysis and life cycle analysis of renewable natural gas production from brewery wastewater via ex-situ methanation processes', *Bioresource Technology*, vol. 422, p. 132234, Apr. 2025, doi: 10.1016/j.biortech.2025.132234.
[29] D. Katla-Milewska, S. M. Nazir, and A. Skorek-Osikowska, 'Synthetic natural gas (SNG) production with higher carbon recovery from biomass: Techno-economic assessment', *Energy Conversion and Management*, vol. 300, p. 117895, Jan. 2024, doi: 10.1016/j.enconman.2023.117895.
[30] B. Batidzirai, G. S. Schotman, M. W. Van Der Spek, M. Junginger, and A. P. C. Faaij, 'Techno-economic performance of sustainable international bio-SNG production and supply chains on short and longer term', *Biofuels Bioprod Bioref*, vol. 13, no. 2, pp. 325–357, Mar. 2019, doi: 10.1002/bbb.1911.
[31] H. Gelten *et al.*, 'Power-to-methanol: Techno-economic analysis of a regional, decentral case-study', *Fuel*, vol. 405, p. 136528, Feb. 2026, doi: 10.1016/j.fuel.2025.136528.
[32] M. Chițoiu, G. Voicu, G. Moiceanu, and P. Tudor, 'ENERGY CONSUMPTION ANALYSIS ON ENERGETIC PLANT BIOMASS GRINDING USING HAMMER MILLS', 2018.
[33] Z. Li and F. Li, 'Study on Performance Optimization of Bag Filter Based on Big Data Analysis', in *2024 3rd International Conference on Energy and Electrical Power Systems (ICEEPS)*, Guangzhou, China: IEEE, Jul. 2024, pp. 1064–1068. doi: 10.1109/ICEEPS62542.2024.10693179.
[34] H. Chen *et al.*, 'Heat exchange and water recovery experiments of flue gas with using nanoporous ceramic membranes', *Applied Thermal Engineering*, vol. 110, pp. 686–694, Jan. 2017, doi: 10.1016/j.applthermaleng.2016.08.191.
[35] Z. Lv, H. Du, S. Xu, T. Deng, J. Ruan, and C. Qin, 'Techno-economic analysis on CO2 mitigation by integrated carbon capture and methanation', *Applied Energy*, vol. 355, p. 122242, Feb. 2024, doi: 10.1016/j.apenergy.2023.122242.
[36] X. Cui, G. Song, A. Yao, H. Wang, L. Wang, and J. Xiao, 'Technical and Economic Assessments of a novel biomass-to-synthetic natural gas (SNG) process integrating O2-enriched air gasification', *Process Safety and Environmental Protection*, vol. 156, pp. 417–428, Dec. 2021, doi: 10.1016/j.psep.2021.10.025.